


Cytoplasmic liver kinase B1 promotes the growth of human lung adenocarcinoma by enhancing autophagy

Mengjie Liu¹  | Lili Jiang¹ | Xiao Fu¹ | Wenjuan Wang¹ | Jiequn Ma² | Tao Tian¹ | Kejun Nan¹ | Xuan Liang¹

¹Department of Medical Oncology, First Affiliated Hospital of Xi'an Jiaotong University, Xi'an, China

²1st Department of Medical Oncology, Shaanxi Provincial Cancer Hospital, Xi'an, China

Correspondence: Xuan Liang and Kejun Nan, Department of Oncology, The First Affiliated Hospital, College of Medicine, Xi'an Jiaotong University, 277 Yanta West Road, Xi'an, Shaanxi 710061, China. (elva_0209@126.com); (nankj@163.com).

Funding information

National Natural Science Foundation of China, Grant/Award Number: 81502099

Liver kinase B1 (*LKB1*) as a tumor suppression gene that is associated with various kinds of cancers, including lung cancer. In this study, we found that the effect of *LKB1* on tumor growth was dependent on its subcellular expression in A549 and HCC827 cells. Full-length *LKB1* decreased the proliferation and clonogenicity of A549-*LKB1* and HCC827-*LKB1* cells, but increased their apoptosis. Opposite effects were observed in A549-*LKB1_s* and HCC827-*LKB1_s* cells that overexpressed truncated *LKB1* without the nuclear localization sequence. The truncated cytoplasmic *LKB1* enhanced the growth of implanted tumors in vivo. The truncated cytoplasmic *LKB1* promoted autophagy, which was independent of AMP-activated protein kinase and mTOR signaling in A549 and HCC827 cells. Further characterization indicated that higher levels of cytoplasmic *LKB1* expression were associated with advanced TNM stage and reduced overall survival (OS) in 190 patients with adenocarcinoma. In contrast, high nuclear expression of *LKB1* is associated with early TNM stage and longer OS. The high level of cytoplasmic *LKB1* expression was an independent risk factor for poor overall survival in patients with adenocarcinoma. Together, our results revealed that cytoplasmic *LKB1* promotes the growth of lung adenocarcinoma and could be a prognostic marker for lung adenocarcinoma.

KEYWORDS

autophagy, *LKB1*, lung adenocarcinoma, proliferation, subcellular expression

1 | INTRODUCTION

Nonsmall cell lung cancer (NSCLC) is one of the most common malignant tumors and has a high mortality rate.¹ The incidence of NSCLC is increasing worldwide. Although significant progression has been made in the diagnosis of NSCLC, a portion of NSCLC patients are diagnosed with advanced TNM stage at the first visit. Therefore, it is important to explore the possible molecular pathogenesis and prognosis biomarkers of NSCLC.

Liver kinase B1 (*LKB1*) was also known as *STK11*.² Germline mutation of *LKB1* is associated with Peutz-Jeghers syndrome, an autosomal dominant inherited disease, which is prone to many kinds of malignant tumors.³ *LKB1* contains three domains, the central kinase domain, the carbon terminal domain, and the nitrogen terminal domain. The central kinase domain is highly conservative. Most Peutz-Jeghers syndrome-related mutations occur in this region. The carbon terminal domain is the posttranscriptional modification region. It contains 4 autophosphorylation sites, 4 phosphorylation sites, and 1 farnesylation site. The nuclear localization signal locates in the nitrogen terminal domain. It regulates the subcellular localization of *LKB1*. Previous studies have found that somatic mutation of

Nan and Liang contributed equally to this work.

This is an open access article under the terms of the Creative Commons Attribution-NonCommercial-NoDerivs License, which permits use and distribution in any medium, provided the original work is properly cited, the use is non-commercial and no modifications or adaptations are made.

© 2018 The Authors. *Cancer Science* published by John Wiley & Sons Australia, Ltd on behalf of Japanese Cancer Association.

LKB1 occurs in many types of sporadic cancers, such as lung cancer,⁴ breast cancer,⁵ and pancreatic cancer,⁶ suggesting that *LKB1* acts as a tumor suppressor. Inactivation of *LKB1* and altered levels of *LKB1* expression are detected in NSCLC tissues.⁷ However, it is unclear what the function of different subcellular *LKB1* is in NSCLC.

Autophagy is an intracellular process of cytoplasmic component degradation in the lysosome to renew some organelles and maintain metabolic homeostasis.^{8,9} During the process of autophagy, stimuli can initiate the formation of autophagosome, a double-membraned vesicle containing cytoplasmic contents and organelles, and its outer membrane will fuse with a lysosome to form an autolysosome to degrade the contents.¹⁰ Autophagy can regulate cell proliferation, apoptosis, and drug sensitivity in tumor cells.¹¹ However, the precise

effects underlying the regulation of autophagy on proliferation and apoptosis of NSCLC are still unclear. Furthermore, *LKB1* acts as an upstream kinase for AMP-activated protein kinase (AMPK) and PI3K/AKT/mTOR signaling.¹² It is poorly understood how the cytoplasmic and nuclear *LKB1* and related signaling regulate the autophagy, proliferation, and apoptosis of NSCLC cells.

2 | MATERIALS AND METHODS

2.1 | Patients

One hundred and ninety patients with lung adenocarcinoma were recruited from the First Affiliated Hospital of Xi'an Jiao Tong

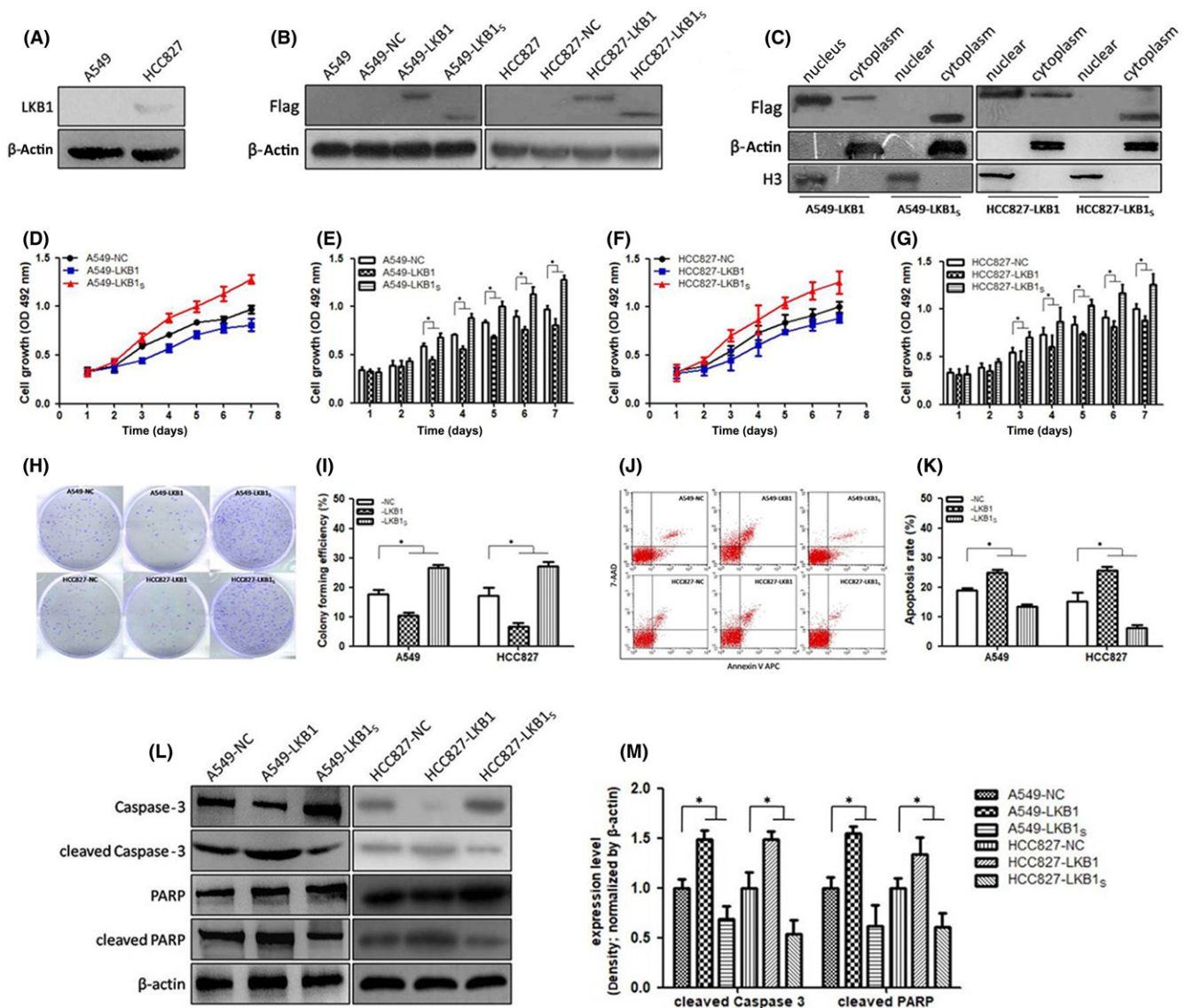


FIGURE 1 Cytoplasmic liver kinase B1 (*LKB1*) promotes proliferation and clonogenicity, but inhibits apoptosis of A549 and HCC827 cells. Distribution and levels of *LKB1* expression in A549-NC, A549-LKB1, A549-LKB1_S, HCC827-NC, HCC827-LKB1, and HCC827-LKB1_S cells, as well as the relative levels of cleaved caspase-3 and poly(ADP-ribose) polymerase (PARP) in individual groups were determined by western blot analysis. The proliferation and clonogenicity of individual groups were tested by MTT and colony forming assays, respectively. The percentages of apoptotic cells were determined by flow cytometry. A,B, Expression of *LKB1*. C, Distribution of *LKB1*. D-G, Cell proliferation. H,I, Cell clonogenicity. J,K, Percentages of apoptotic cells. L,M, Levels of apoptosis-related proteins. * $P < .05$. NC, negative control

University (Xi'an, China) from December 2009 to December 2012. Individual patients were diagnosed with lung adenocarcinoma by pathology in a blinded manner. The patients received thoracotomy or lobectomy to remove the whole tumors without adjuvant chemotherapy or radiotherapy before surgery. The tumor specimens were staged according to the 8th edition of the American Joint Committee on Cancer classification system. Those patients were followed up until December 2016.

2.2 | Immunohistochemical staining

The freshly dissected human lung adenocarcinoma and mouse transplanted tumors were fixed in 10% buffered formalin overnight and paraffin-embedded. The tumor tissue sections (5 μ m) were deparaffinized and rehydrated, followed by antigen retrieval in a microwave oven. The sections were incubated in 3% hydrogen peroxide in methanol for 10 minutes to inactivate endogenous peroxidase,

blocked with 10% normal goat serum for 20 minutes at room temperature, and incubated with anti-LKB1 (1:200 dilution, D60C5F10; Cell Signaling Technology, Danvers, MA, USA) and anti-Ki67 (1:200 dilution, 8D5; Cell Signaling Technology) at 4°C overnight. After being washed, the sections were incubated with secondary antibody and then with HRP-conjugated avidin for 30 minutes at room temperature, visualized with 3,3'-diaminobenzidine tetrahydrochloride, then counterstained with hematoxylin. These stained signals were photographed under a microscope (Q550CW; Leica, Manheim, Germany). The intensity of staining was evaluated semiquantitatively as scores of: 0, not staining; 1, faint staining; 2, moderate staining; and 3, strong staining. The percentages of stained cells were examined and defined as: 0, <5%; 1, 5%-25%; 2, 26%-50%; 3, 51%-75%; and 4, >75%. The final scores of each section were calculated by multiplying these two numbers, resulting in a score of 0-12. The samples with a score of 1-5 were defined as having low levels of expression; samples with a score of 6-12 were defined as having high levels of

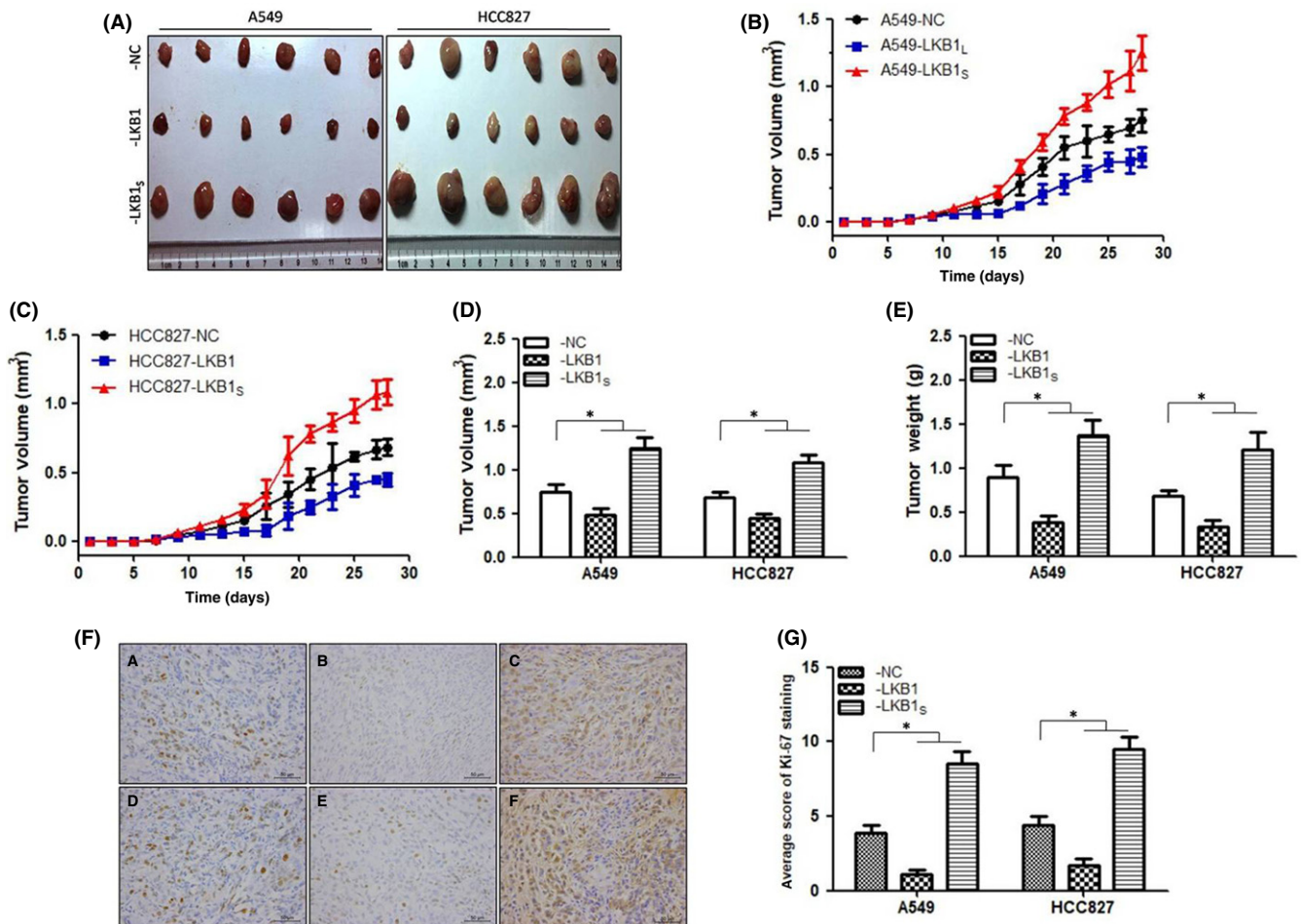


FIGURE 2 Cytoplasmic liver kinase B1 (*LKB1*) promotes the growth of implanted lung tumors in mice. BALB/c nude mice were randomized and implanted s.c. with equal numbers of A549-LKB1, A549-LKB1_s, A549-NC, HCC827-LKB1, HCC827-LKB1_s, or HCC827-NC cells, and the dynamic growth of individual groups of tumors was monitored up to 28 days. Tumors were then dissected out and measured for their volumes and weights. Levels of Ki67 expression in individual tumors were determined by immunohistochemistry. A, Representative tumors. B, C, Dynamic growth of implanted tumors. D, Volumes of tumors. E, Weights of tumors. F, Levels of Ki67 expression in tumors. a, A549-NC tumor; b, A549-LKB1 tumor; c, A549-LKB1_s tumor; d, HCC827-NC tumor; e, HCC827-LKB1 tumor; f, HCC827-LKB1_s tumor. G, Scores of Ki-67 expression in each group. **P* < .05. NC, negative control

expression. The intensity of nuclear anti-LKB1 staining was defined as: 0, no staining; 1, staining. The percentages of nuclear-stained cells were defined as 0, <5%; 1, 5%-37%; 2, 38%-70%; and 3, >70%. A final score of <1 was defined as no nuclear LKB1 expression, whereas a final score of >2 was defined as expressing nuclear LKB1.

2.3 | Cell culture and transfection

Human lung adenocarcinoma A549 and HCC827 cells were cultured in DMEM containing 10% (v/v) FBS at 37°C in 5% CO₂. All the vectors contained the kanamycin/G418 resistance gene. When the cells reached 70% confluency, they were transfected with individual expression plasmids using the TurboFect transfection reagent (Thermo, Waltham, MA, USA). The plasmids included C-Flag pcDNA3-LKB1 for expression of the whole length of LKB1, C-Flag pcDNA3-LKB1_s for the expression of LKB1 without nuclear

localization signal, or control pcDNA3 (Addgene, Cambridge, MA, USA). Two days later, these transfected cells were treated with 500 µg/mL G418 for 21 days to establish the stable expression cell lines A549-LKB1, A549-LKB1_s, A549-NC, HCC827-LKB1, HCC827-LKB1_s, and HCC827-NC. In addition, the different groups of cells were treated with, or without, 10 mmol/L 3-methyladenine (3-MA), 40 µmol/L compound C, or 10 µmol/L MHY1485 (Sigma, Burlington, MA, USA) to inhibit autophagy, AMPK, or mTOR, respectively.

2.4 | Western blot analysis

The different groups of cells were lysed in RIPA lysis buffer (Beyotime Chemical, Beijing, China). In addition, nuclear and cytoplasm proteins were extracted from the different groups of cells using the Nuclear and Cytoplasmic Protein Extraction Kit (Beyotime Chemical). After quantification of protein concentrations, the protein samples

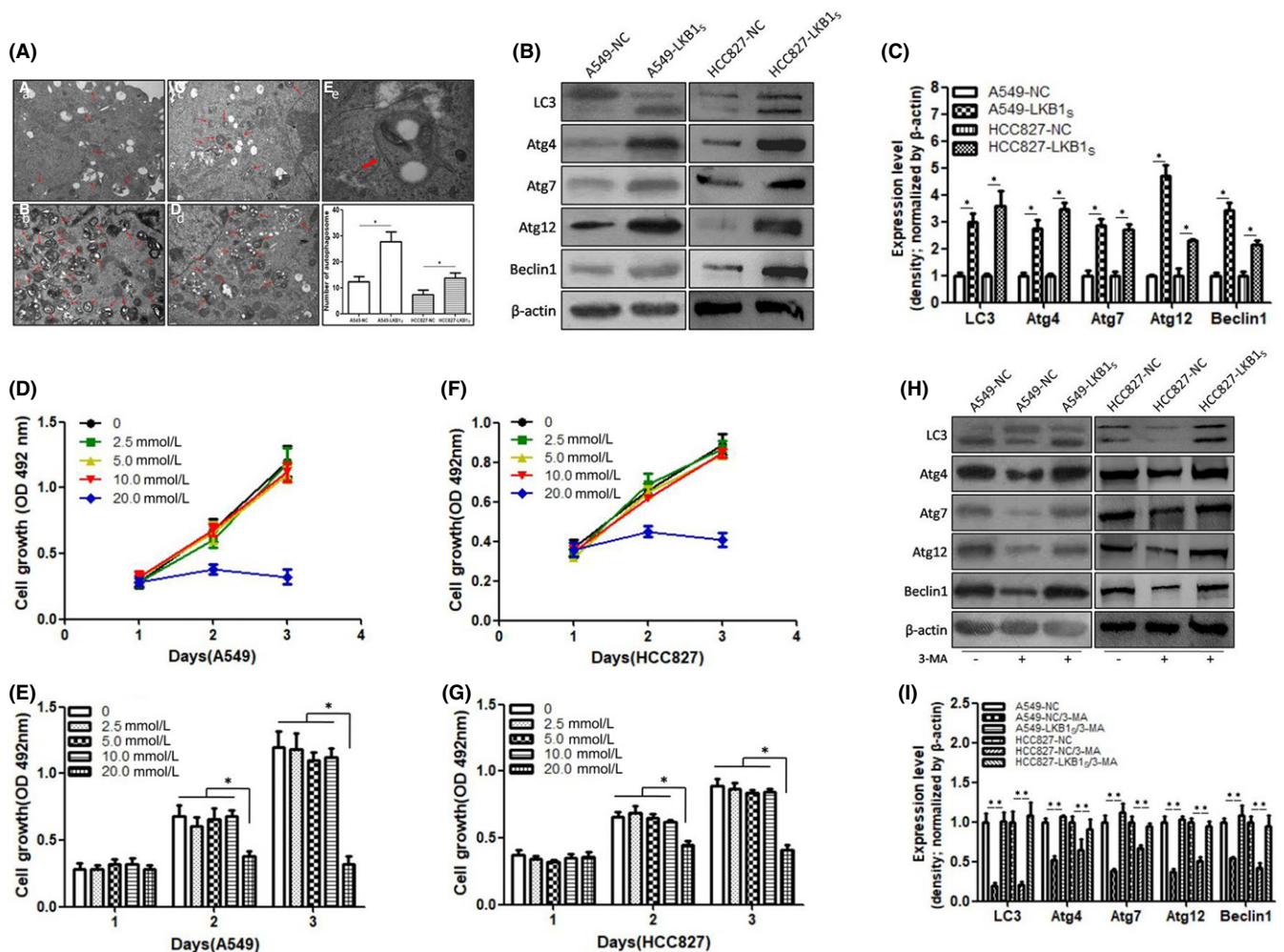


FIGURE 3 Cytoplasmic liver kinase B1 (LKB1) increases autophagy in A549 and HCC827 cells. Numbers of autophagosomes in A549-NC, A549-LKB1_s, HCC827-NC, and HCC827-LKB1_s cells were characterized by transmission electron microscopy (TEM), and the relative levels of autophagy-related molecule expression were determined by western blot analysis. A549 and HCC827 cells were treated with the indicated doses of 3-methyladenine (3-MA) for varying time periods, and the viability of individual groups of cells was determined by MTT. The sensitivity of A549-NC, A549-LKB1_s, HCC827-NC, and HCC827-LKB1_s cells to 3-MA was determined for the relative levels of autophagy-related molecule expression by western blot. A, TEM analysis of autophagosomes. a, A549-NC cells (×20 000); b, A549-LKB1_s cells (×20 000); c, HCC827-NC cell (×20 000); d, HCC827-LKB1_s cell (×20 000); e, autophagosome (×50 000). B,C, Autophagy-associated molecule expression. D-G, Effect of 3-MA on A549 and HCC827 cells. H-I, Western blot analysis of autophagy-associated molecule expression. **P* < .05. NC, negative control

(20–50 $\mu\text{g}/\text{lane}$) were separated by SDS-PAGE on 8%–12% gels and transferred onto PVDF membranes (Millipore, Billerica, MA, USA). After being blocked with 5% fat-free milk powder in TBST, the membranes were incubated with primary antibodies against Beclin1 (ePR1733Y, 1:800 dilution; Abcam, Cambridge, UK), LC3 (L7543, 1:1000 dilution; Sigma), Atg4 (D62C10, 1:1000 dilution; Cell Signaling Technology), Atg7 (D12B11, 1:1000 dilution; Cell Signaling Technology), Atg12 (D88H11, 1:1000 dilution; Cell Signaling Technology), cleaved caspase-3 (5A1E, 1:1000 dilution; Cell Signaling Technology), caspase-3 (8G10, 1:1000 dilution; Cell Signaling Technology), cleaved poly(ADP-ribose) polymerase (PARP) (19F4, 1:1000 dilution; Cell Signaling Technology), PARP (46D11, 1:1000 dilution; Cell Signaling Technology), H3 (1B1B2, 1:1000 dilution; Cell Signaling Technology), and β -actin (sc-130301, 1:1000 dilution; Santa Cruz Biotechnology, Santa Cruz, CA, USA) at 4°C overnight. After being washed, the bound antibodies were detected with HRP-conjugated secondary antibodies and visualized using the enhanced chemiluminescent reagents (Millipore). The relative levels of target protein were determined by Biolmaging Systems (ChemiDoc-It 415 Imager, UVP; Upland, CA, USA).

2.5 | Cell proliferation assay

The different groups of cells (2×10^3 cells/well) were cultured in 96-well plates overnight, and the proliferation of each group of cells was determined by MTT assay. Briefly, each well of cells was exposed to 5 mg/mL MTT for 6 hours daily for 7 days and the generated formazan in individual wells was solubilized by adding 150 μL DMSO, followed by measuring the optical density at 492 nm in a microplate reader. The experiments were carried out in triplicate, and control and experimental cells were tested simultaneously.

2.6 | Colony formation assay

The different groups of cells (800 cells/well) were cultured in triplicate in 6-well plates in DMEM containing 10% (v/v) FBS at 37°C in 5% CO_2 for 21 days. The visible clones were fixed by 4% paraformaldehyde for 15 minutes and stained with 0.1% crystal violet for 30 minutes. The numbers of formed clones in individual wells were counted in a blinded manner.

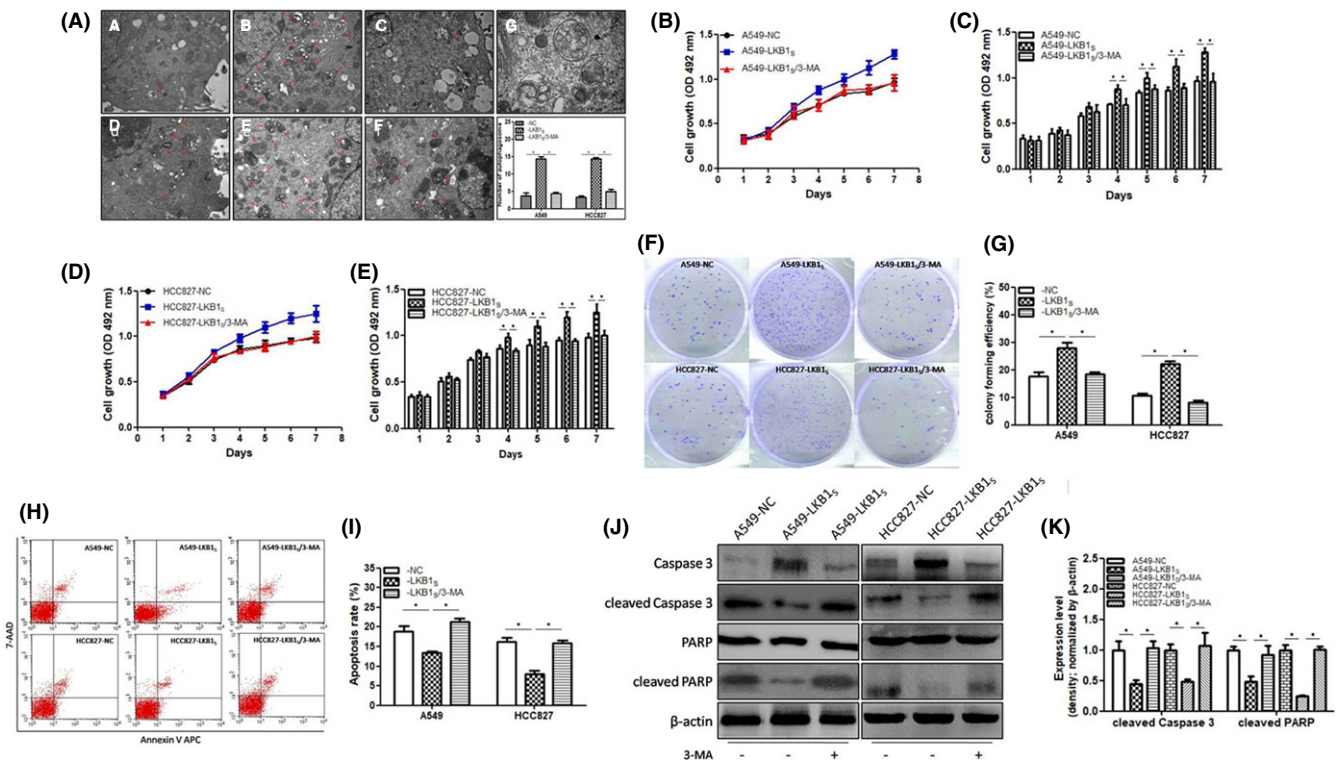


FIGURE 4 Inhibition of autophagy abrogates the cytoplasmic liver kinase B1 (LKB1)-enhanced proliferation and clonogenicity of A549 and HCC827 cells. Numbers of autophagosomes in A549-NC, A549-LKB1_s, A549-LKB1_s/3-methyladenine (3-MA), HCC827-NC, HCC827-LKB1_s, and HCC827-LKB1_s/3-MA cells were characterized by transmission electron microscopy (TEM). Proliferation and clonogenicity of individual groups of cells were tested by MTT and colony forming assays, respectively. Percentages of apoptotic cells were determined by flow cytometry. Relative levels of cleaved caspase-3 and poly(ADP-ribose) polymerase (PARP) in individual groups of cells were determined by western blot analysis. A, TEM analysis of autophagosomes. a, A549-NC cells ($\times 20\,000$); b, A549-LKB1_s cells ($\times 20\,000$); c, A549-LKB1_s/3-MA cells ($\times 20\,000$); d, HCC827-NC cells ($\times 20\,000$); e, HCC827-LKB1_s cell ($\times 20\,000$); f, HCC827-LKB1_s/3-MA cells ($\times 20\,000$); g, autophagosome ($\times 50\,000$). B–E, MTT assay for proliferation. F, G, Numbers of clones. H, I, Percentages of apoptotic cells. J, K, Western blot analysis of the levels of apoptosis-related proteins. * $P < .05$. NC, negative control

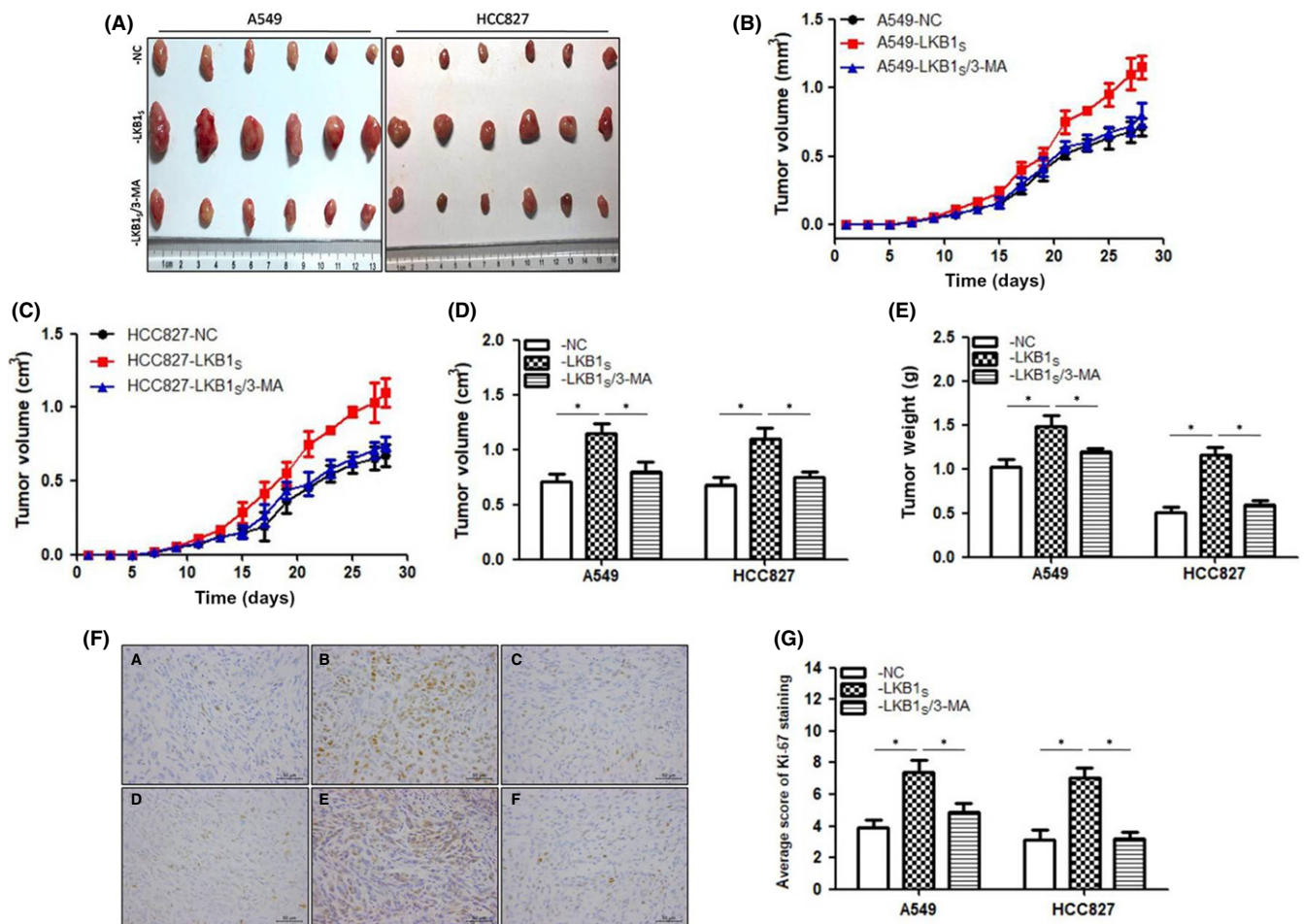


FIGURE 5 Inhibition of autophagy reduced the cytoplasmic liver kinase B1 (*LKB1*)-enhanced growth of implanted lung tumors in mice. BALB/c nude mice were randomized and implanted with the same numbers of A549-NC, A549-*LKB1_s*, HCC827-NC, or HCC827-*LKB1_s* cells and the mice bearing A549-*LKB1_s* and HCC827-*LKB1_s* tumors were randomized and injected with PBS or 3-methyladenine (3-MA). The dynamic growth of individual groups of tumors was monitored up to 28 days. Tumors were then dissected out and measured for their volumes and weights. Levels of Ki67 expression were determined by immunohistochemistry. A, Representative tumors. B,C, Dynamic growth of implanted tumors. D, Volumes of tumors. E, Weights of tumors. F, Levels of Ki67 expression. a, A549-NC tumor; b, A549-*LKB1_s* tumor; c, A549-*LKB1_s*/3-MA tumor; d, HCC827-NC tumor; e, HCC827-*LKB1_s* tumor; f, HCC827-*LKB1_s*/3-MA tumor. G, Ki-67 expression scores in each group. * $P < .05$. NC, negative control

2.7 | Flow cytometry

The percentages of apoptotic cells in each group were determined by flow cytometry using the Annexin V Apoptosis Detection Kit (88-8007; Thermo Fisher Scientific, Waltham, MA, USA). Briefly, the different groups of cells (10^5 /tube) were stained in duplicate with 5 μ L annexin V-allophycocyanin and 5 μ L 7-AAD solutions for 15 minutes at room temperature. After being washed, the percentages of apoptotic cells were determined by flow cytometry and analyzed using the FlowJo (FlowJo LLC, Ashland, OR, USA) software.

2.8 | Transmission electron microscopy

Autophagosomes in individual cells were detected by transmission electron microscopy (TEM). Briefly, the cells were harvested and the cell pellets were fixed by 2.5% glutaraldehyde for 2 hours at 4°C. After dehydrated by acetone, these cell pellets were embedded and

placed in 65°C for 2 hours. The cell ultrathin sections (50-70 nm) were stained by sodium acetate and lead citrate, then observed under using TEM. Autophagosomes were counted in 5 high power fields ($\times 20\,000$) to obtain the average number of autophagosomes for each sample.

2.9 | Lung cancer xenograft in nude mice

Male BALB/c nude mice at 4 weeks of age were purchased from the Animal Center of Xi'an Jiaotong University and housed in a specific pathogen-free facility with free access to autoclaved food and water. To establish xenograft tumors, individual mice were randomized and implanted s.c. with 1×10^6 A549-NC, A549-*LKB1*, A549-*LKB1_s*, HCC827-NC, HCC827-*LKB1*, or HCC827-*LKB1_s* cells ($n = 6$) in 100 μ L DMEM/Matrigel (No. 356234; BD, Franklin Lakes, NJ, USA) into their back. In addition, another set of mice were randomized and implanted s.c. with 1×10^6 A549-NC, A549-*LKB1_s*, HCC827-

NC, or HCC827-LKB1_s cells. When a visible tumor was established, the mice bearing A549-LKB1_s and HCC827-LKB1_s cells were randomized and injected intratumorally with 100 μ L PBS as the A549-LKB1_s and HCC827-LKB1_s group or with 5 mmol/L 3-MA (M9281; Sigma) every other day for 2 weeks. The growth of implanted tumors was monitored every other day for their volumes that were calculated using the formula: $V = 0.5 \times \text{length} \times \text{width}^2$.

2.10 | Statistical analysis

Data are expressed as the mean \pm SD or real case number. The association between percent cases with positive staining and clinical parameters was analyzed by Pearson's χ^2 test. Overall survival (OS), defined as time from diagnosis to death or to the last follow-up, was used to draft survival curves. Survival rates were estimated by the Kaplan-Meier method, and the difference between subgroups was tested by the log-rank test. The potential factors for OS were determined by univariate and multivariate analyses. The difference among groups was analyzed by repeated ANOVA, and the difference between groups was analyzed by Student's *t* test. All statistical analyses were carried out using SPSS 22.0 software (International Business Machines Corporation, Armonk, NY, USA). *P*-value < .05 was considered statistically significant.

3 | RESULTS

3.1 | LKB1 regulates proliferation of A549 and HCC827 cells, dependent on its subcellular localization

LKB1 has been considered to be a tumor suppressor. To determine the role of different subcellular localizations of LKB1 in regulating A549 and HCC827 cell proliferation, A549 and HCC827 cells were transfected with vehicle, the plasmid for expressing full-length LKB1, or the plasmid for expressing LKB1 without the nuclear localization sequence to generate stably expressing A549-NC, HCC827-NC, A549-LKB1, HCC827-LKB1, A549-LKB1_s, or HCC827-LKB1_s cells. Western blot analysis indicated that A549 cells did not express endogenous LKB1 and HCC827 cell expressed low levels of endogenous LKB1 (Figure 1A). A549-LKB1, HCC827-LKB1, A549-LKB1_s, and HCC827-LKB1_s expressed the flag-fused LKB1 with different sizes, as expected (Figure 1B). Although LKB1 was expressed in both the cytoplasm and nucleus of A549-LKB1 and HCC827-LKB1 cells, LKB1 was only detected in the cytoplasm of A549-LKB1_s and HCC827-LKB1_s cells (Figure 1C). The MTT assays indicated that the proliferation of A549-LKB1 cells was weaker than that of A549-NC cells, whereas the proliferation of A549-LKB1_s cells was significantly stronger than that of A549-NC (Figure 1D,E). The same results were found in HCC827 cells (Figure 1F,G). Similarly, colony formation assays revealed that the percentages of A549-LKB1 or HCC827-LKB1 cells that formed clones were significantly less than that of A549-NC or HCC827-NC cells, respectively, whereas the percentages of A549-LKB1_s or HCC827-LKB1_s cells that formed clones

were significantly greater than that of A549-NC or HCC827-NC cells, respectively (Figure 1H,I). In addition, flow cytometry analysis showed that the percentages of apoptotic A549-NC or HCC827-NC cells were significantly less than that of A549-LKB1 or HCC827-LKB1 cells, but higher than that of A549-LKB1_s or HCC827-LKB1_s cells (Figure 1J,K). Moreover, a similar pattern of the relative levels of cleaved caspase-3 and PARP was detected in these cell lines (Figure 1L,M). Collectively, such data indicated that cytoplasmic LKB1 promoted the proliferation and clonogenicity, but inhibited the apoptosis, of A549 and HCC827 cells in vitro.

To test the effect of LKB1 in vivo, A549-LKB1, A549-LKB1_s, A549-NC, HCC827-LKB1, HCC827-LKB1_s, and HCC827-NC cells were implanted s.c. into nude mice and the growth of implanted tumors was monitored for 28 days (Figure 2A). The dynamic growth of A549-NC tumors was faster than that of A549-LKB1 tumors, but slower than that of A549-LKB1_s tumors. The tumor weights and volumes in the A549-NC tumors were significantly less than that of A549-LKB1_s tumors, but greater than that of A549-LKB1 tumors. The same results were found in HCC827 cells (Figure 2B-E). Further immunohistochemistry revealed that the A549-NC tumors showed moderate levels of anti-Ki67 staining, whereas the levels of anti-Ki67 staining in the A549-LKB1 tumors were obviously diminished. In contrast, the levels of anti-Ki67 staining in A549-LKBs tumors were stronger than that of A549-NC tumors. A similar pattern of the relative levels of Ki67 was detected in HCC827 cells (Figure 2F,G). Collectively, such data indicated that cytoplasmic LKB1 promoted the tumor formation of A549 and HCC827 cells in vivo.

3.2 | Cytoplasmic LKB1 promotes autophagy and proliferation of A549 and HCC827 cells

To understand the potential mechanisms underlying the effect of cytoplasmic LKB1, we characterized autophagy in A549-LKBs, HCC827-LKB1_s, and their control cells, A549-NC and HCC827-NC, by TEM. We found that the number of autophagosomes in A549-LKB1_s or HCC827-LKB1_s cells was significantly higher than that in A549-NC or HCC827-NC cells (Figure 3A). Further analysis indicated that the relative levels of LC3II, Beclin1, Atg4, Atg7, and Atg12 in A549-LKB1_s or HCC827-LKB1_s cells were significantly higher than that in A549-NC or HCC827-NC cells (Figure 3B,C). To further confirm the effect of LKB1_s on cell autophagy, we used 10 mmol/L 3-MA (Figure 3D-G) to inhibit autophagy of A549-NC and HCC827-NC cells. The relative levels of LC3II, Beclin1, Atg4, Atg7, and Atg12 expression in A549-NC or HCC827-NC cells treated with 3-MA were significantly reduced compared with A549-NC or HCC827-NC cells. Compared with A549-NC or HCC827-NC cells treated with 3-MA, the relative expression levels of those molecules in the A549-LKBs cells that had been treated with 3-MA were restored (Figure 3H,I). These results suggested that cytoplasmic LKB1 promoted autophagy in A549 and HCC827 cells.

We further uncovered the effect of cytoplasmic LKB1 reduced autophagy on cell growth in A549 and HCC827 cells. We found that the number of autophagosomes in A549-LKB1_s or HCC827-LKB1_s

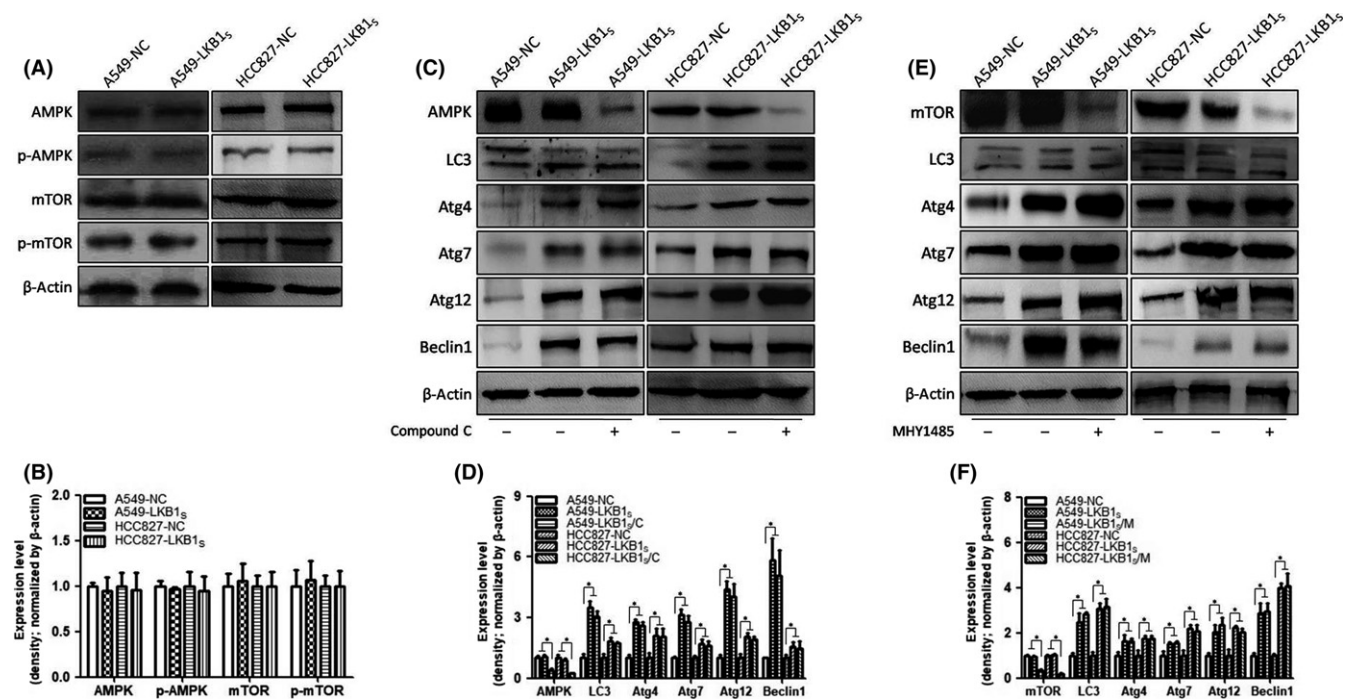


FIGURE 6 Cytoplasmic liver kinase B1 (LKB1) promotes autophagy, independent of AMP-activated protein kinase/mTOR signaling in A549 and HCC827 cells. A549-LKB1_s and HCC827-LKB1_s cells were treated with, or without, compound C or MHY1485, and the levels of autophagy-related molecule expression in those cells were determined by western blot analysis. A,B Relative levels of autophagy-related molecule expression in A549-NC, A549-LKB1_s, HCC827-NC, and HCC827-LKB1_s cells. C,D, Relative levels of autophagy-related molecule expression in A549-NC, A549-LKB1_s, compound C-treated A549-LKB1_s, HCC827-NC, HCC827-LKB1_s, and compound C-treated HCC827-LKB1_s cells. E,F, Relative levels of autophagy-related molecule expression in A549-NC, A549-LKB1_s, MHY1485-treated A549-LKB1_s, HCC827-NC, HCC827-LKB1_s, and MHY1485-treated HCC827-LKB1_s cells. * $P < .05$. NC, negative control; p-, phosphorylated

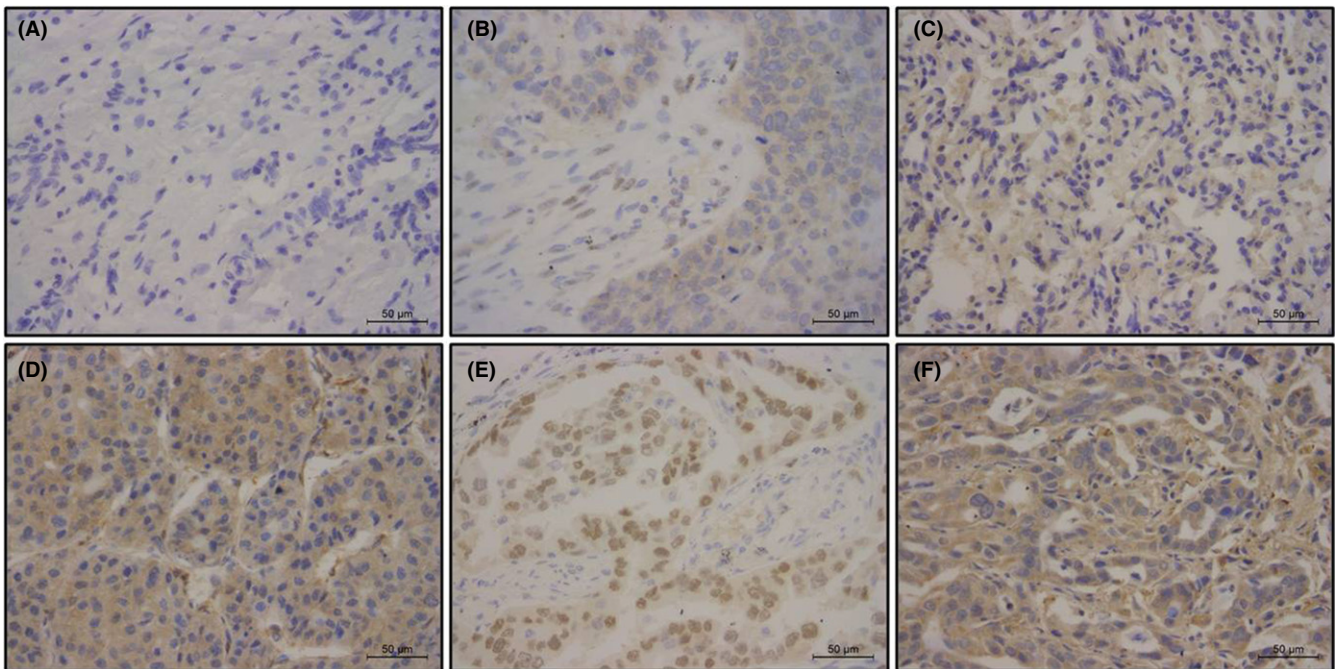


FIGURE 7 Immunohistochemistry analysis of liver kinase B1 (LKB1) expression in lung adenocarcinoma. A, No cytoplasmic anti-LKB1 staining. B, Faint cytoplasmic anti-LKB1 staining. C, Moderate cytoplasmic anti-LKB1 staining. D, Strong cytoplasmic anti-LKB1 staining. E, Samples with nuclear anti-LKB1 staining. F, Samples without nuclear anti-LKB1 staining

TABLE 1 Distribution of *LKB1* expression in 190 lung adenocarcinoma tissues

Intensity	All, N = 190	
	n	%
<i>LKB1</i> : cytoplasm staining		
Low		
0	29	15.2
1	92	47.9
High		
2	61	32.1
3	9	4.7
<i>LKB1</i> : nuclear staining		
0	129	68.2
1	61	31.8

TABLE 2 Quantitative analysis of *LKB1* in 190 lung adenocarcinoma tissues

	<i>LKB1</i> : nuclear staining				Test
	0 (n = 129)		1 (n = 61)		
<i>LKB1</i> : cytoplasm staining	N	%	N	%	<i>P</i> = .037
Low (n = 120)	75	58.1	45	73.8	
High (n = 70)	54	41.9	16	26.2	

cells treated with 3-MA was less than that of A549-LKB1_s or HCC827-LKB1_s cells (Figure 4A). Likewise, inhibition of autophagy by 3-MA significantly inhibited the proliferation of A549-LKB1_s or HCC827-LKB1_s cells (Figure 4B-E). A similar pattern of clonogenicity and apoptosis was detected in different groups of cells (Figure 4F-I). Western blot analysis indicated that the relative levels of cleaved caspase-3 and PARP in the 3-MA-treated A549-LKB1_s and HCC827-LKB1_s cells were similar to that of A549-NC and HCC827-NC cells, which were significantly lower than that in A549-LKB1_s and HCC827-LKB1_s cells without 3-MA treatment (Figure 4J,K).

Next, we found that, in comparison with A549-LKB1_s or HCC827-LKB1_s cells, inhibition of autophagy significantly inhibited the growth of implanted A549-LKB1_s or HCC827-LKB1_s tumors (Figure 5A-C). Inhibition of autophagy also significantly reduced the tumor volumes and weights in mice (Figure 5D,E). Moreover, immunohistochemistry revealed that inhibition of autophagy obviously decreased Ki67 expression in the tumor tissues (Figure 5F,G). Together, these data indicated that cytoplasmic *LKB1* promoted autophagy, which was associated with enhanced proliferation in A549 and HCC827 cells.

3.3 | Autophagy enhanced by cytoplasmic *LKB1* is independent of AMPK/mTOR signaling in A549 and HCC827 cells

It is well known that AMPK/mTOR signaling regulates autophagy, particularly in a nutrition-deficient condition.¹³ To further understand

the regulation of cytoplasmic *LKB1* on autophagy, the relative levels of AMPK and mTOR were determined by western blot analysis. We found that there were similar levels of AMPK and mTOR expression and phosphorylation between A549-NC or HCC827-NC and A549-LKB1_s or HCC827-LKB1_s cells (Figure 6A,B), suggesting that induction of unipolar cytoplasmic *LKB1* expression did not alter AMPK and mTOR signaling in A549 and HCC827 cells. Furthermore, treatment with compound C (an AMPK inhibitor) or with MHY1485 (an mTOR inhibitor) did not change the relative levels of LC3II, Atg4, Atg7, Atg12, or Beclin1 expression in A549-LKB1_s or HCC827-LKB1_s cells (Figure 6C-F). Hence, autophagy enhanced by cytoplasmic *LKB1* was independent of AMPK/mTOR signaling in A549 and HCC827 cells.

3.4 | Expression of *LKB1* in human lung adenocarcinoma

We finally examined *LKB1* expression in 190 lung adenocarcinoma tissues by immunohistochemistry. There were 162 (84.8%) of 190 lung adenocarcinoma tissues with cytoplasmic *LKB1* expression and 61 (31.8%) with nuclear *LKB1* expression (Figure 7, Table 1). The frequency of cancers with nuclear *LKB1* and low levels of cytoplasmic *LKB1* expression was significantly lower than those without nuclear *LKB1* and high levels of cytoplasmic *LKB1* expression (Table 2). Stratification analysis indicated that cytoplasmic *LKB1* expression was positively associated with T stage (*P* = .01) and TNM stage (*P* = .045; Table 3) in this cohort. Furthermore, the nuclear *LKB1* expression was associated inversely with T stage (*P* = .028) and TNM stage (*P* = .023, Table 3) in this cohort. More importantly, patients with higher levels of cytoplasmic *LKB1*-expressing lung cancer had significantly shorter OS than those with lower levels of cytoplasmic *LKB1*-expressing cancers (Figure 8A, *P* < .001). In contrast, patients with negative nuclear *LKB1*-expressing lung cancers had significantly shorter OS than those with nuclear *LKB1*-expressing cancers (Figure 8B, *P* < .001). Further analysis indicated that the patients with nuclear and lower levels of cytoplasmic *LKB1*-expressing lung cancers had the longest OS and the patients with either lower levels of cytoplasmic *LKB1*, but without nuclear *LKB1*, or nuclear and higher levels of cytoplasmic *LKB1*-expressing lung cancers had similar OS, whereas those with higher levels of cytoplasmic *LKB1*, but without nuclear *LKB1*-expressing lung cancers had the shortest OS in this population (Figure 8C, *P* < .001). Finally, univariate analysis indicated that age at diagnosis (<60 years old), lepidic lung adenocarcinoma, and nuclear *LKB1* expression were associated with a longer OS, whereas advanced T and TNM stages, lymph node metastasis, and cytoplasmic *LKB1* expression were associated with a shorter OS in this cohort (Table 4). Multivariate analysis revealed that age at diagnosis (<60 years old), lepidic lung adenocarcinoma, and nuclear *LKB1* expression were independent factors for a longer OS, whereas advanced TNM stages and cytoplasmic *LKB1* expression were independent risk factors for a shorter OS in this cohort (Table 4). Collectively, our data indicated that subcellular localization of *LKB1* was an independent biomarker for prognosis of patients with lung adenocarcinoma.

TABLE 3 Stratification analysis of the distribution of *LKB1* expression with demographic and clinical characteristics of patients with lung adenocarcinoma

Characteristic	n	%	<i>LKB1</i> expression				P-value	<i>LKB1</i> expression				P-value
			Cytoplasm					Nuclear				
			Low		High			Low		High		
n	%	n	%	n	%	n	%	n	%			
All cases	190											
Gender												
Male	103	54.21	67	65.05	36	34.85	0.557	71	68.93	32	31.07	0.739
Female	87	45.79	53	60.92	34	39.08		58	66.67	29	33.33	
Age, years												
60	104	54.74	61	58.65	43	41.35	0.157	68	65.38	36	34.62	0.385
≥60	86	45.26	59	68.60	27	31.40		62	72.09	25	27.91	
Histological subclassification												
Lepidic	34	17.89	24	70.59	10	29.41	0.633	21	61.76	13	38.24	0.598
Acinar	123	64.74	77	62.60	46	37.40		85	69.11	38	20.89	
Papillary	22	11.58	14	63.64	8	36.36		14	63.64	8	26.36	
Micropapillary	3	1.58	1	33.33	2	66.67		3	100.0	0	0.00	
Solid	8	4.21	4	50.00	4	50.00		6	75.00	2	25.00	
T stage												
T1 + T2	154	81.05	104	67.53	50	32.47	0.010	99	64.29	55	35.71	0.028
T3 + T4	36	18.95	16	44.44	20	55.56		30	83.33	6	16.67	
Lymph node metastasis												
No	102	53.68	68	66.67	34	33.33	0.280	69	67.65	33	32.35	0.937
Yes	88	46.32	52	59.09	36	40.91		60	68.18	28	31.82	
TNM stage												
Stage I-II	118	62.11	81	68.64	37	31.36	0.045	73	61.86	45	38.14	0.023
Stage III-IV	72	37.89	39	54.17	33	45.83		56	77.78	16	22.22	

P-value < .05 are highlighted in bold.

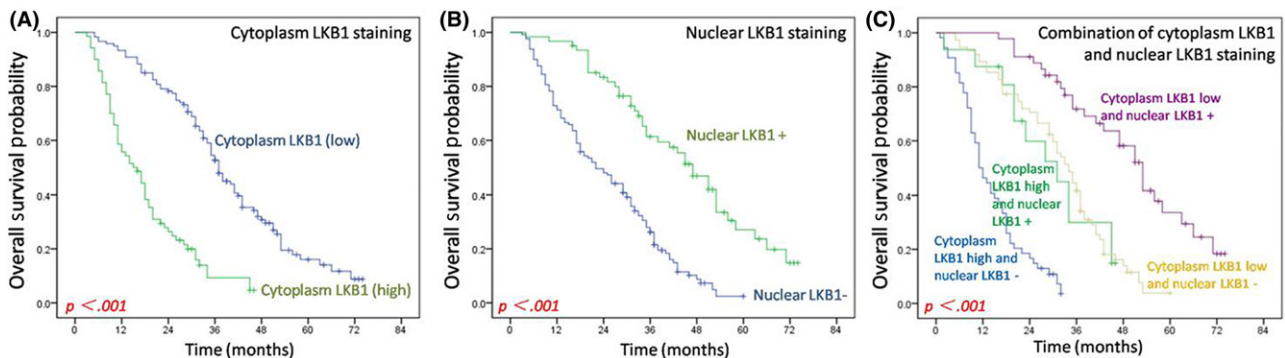


FIGURE 8 High levels of cytoplasmic liver kinase B1 (*LKB1*) expression are associated with poor overall survival in lung adenocarcinoma. Patients with lung adenocarcinoma were stratified, based on the distribution and levels of *LKB1* expression, and their overall survival was established by the Kaplan-Meier method, followed by log-rank test. A, overall survival of low cytoplasmic *LKB1* group and high cytoplasmic *LKB1* group. B, overall survival of positive nuclear *LKB1* group and negative nuclear *LKB1* group. C, overall survival of low cytoplasmic *LKB1* with nuclear *LKB1* group, low cytoplasmic *LKB1* without nuclear *LKB1* group, high cytoplasmic *LKB1* with nuclear *LKB1* group and high cytoplasmic *LKB1* without nuclear *LKB1* group

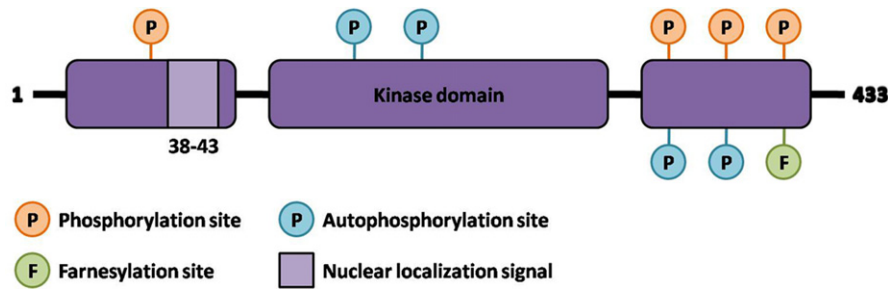


FIGURE 9 Structural diagram of the *LKB1* gene

TABLE 4 Univariate and multivariate analyses of factors affecting overall survival in lung adenocarcinoma patients

Characteristic	n	Univariate analysis		Multivariate analysis	
		HR (95% CI)	P-value	HR (95% CI)	P-value
Gender					
Male	103	1.03 (0.74-1.41)	0.879	–	–
Female	87				
Age, years					
60	104	0.69 (0.50-0.96)	0.027	0.60 (0.42-0.84)	0.003
≥60	86				
Histological subclassification					
Lepidic	34	2.03 (1.29-3.19)	7.17 (3.28-15.63)	2.15 (1.36-3.40)	5.96 (2.70-13.15)
Acinar/papillary	145				
Micropapillary/solid	11				
T stage					
T1 + T2	154	1.57 (1.03-2.38)	0.035	–	–
T3 + T4	36				
Lymph node metastasis					
No	102	1.53 (1.11-2.11)	0.009	–	–
Yes	88				
TNM stage					
Stage I-II	118	2.22 (1.59-3.01)	<0.001	2.02 (1.15-3.56)	0.015
Stage III-IV	72				
Cytoplasmic <i>LKB1</i>					
Low	120	3.89 (2.72-5.56)	<0.001	4.27 (2.88-6.33)	<0.001
High	70				
Nuclear <i>LKB1</i>					
Low	129	0.31 (0.21-0.46)	<0.001	0.27 (0.17-0.40)	<0.001
High	61				

P-value < .05 are highlighted in bold.

–, not applicable; CI, confidence interval; HR, hazard ratio.

4 | DISCUSSION

In this study, we found that cytoplasmic *LKB1* promoted the growth of lung adenocarcinoma by enhancing autophagy. First, we showed that induction of truncated *LKB1*_s was exclusively expressed in the cytoplasm, and full-length *LKB1* was expressed in both cytoplasm and nucleus of A549 and HCC827 cells. *LKB1*_s promoted the proliferation, clonogenicity, and growth of implanted tumors, accompanied

by the inhibition of apoptosis in A549 and HCC827 cells. *LKB1* had opposite effects in A549 and HCC827 cells. Second, we detected higher levels of autophagy in A549-*LKB1*_s or HCC827-*LKB1*_s than the control A549-NC or HCC827-NC cells. Inhibition of autophagy abrogated the effect of *LKB1*_s on the proliferation and clonogenicity of A549 and HCC827 cells. Such data clearly indicated that cytoplasmic *LKB1*_s promoted autophagy and growth of lung adenocarcinoma cell.

The relationship between autophagy and cancer is complicated. Previous studies have found low levels of autophagy in cancer cells due to the mutation, deletion, and functional inhibition of autophagy-related genes.¹⁴ Autophagy can inhibit the process of carcinogenesis by degrading harmful proteins and damaged organelles, reducing the instability of the genome, or converging inflammatory responses induced by necrosis.¹⁵ Inhibition of autophagy is associated with promoting cell differentiation, protein catabolism, and autophagic cell death.¹⁶ However, our findings could be surprisingly against the traditional dogma. It is possible that autophagy induced by LKB1_s may help cancer cell survival under a nutrition deficiency circumstance to overcome metabolic stress and maintain energy balance.

It is well known that LKB1 can activate AMPK. Activation of AMPK can inhibit mTOR and further enhance autophagy.¹⁷ In this study, we found that cytoplasmic LKB1_s enhanced autophagy, independent of AMPK and mTOR signaling. The full-length LKB1 localizes in the nucleus. It interacts with STe20 Related Adaptor in the nucleus to form a dipolymer complex and the complex relocates from the nucleus to the cytoplasm where the complex binds to MO25 and forms a tripolymer complex, leading to AMPK activation.¹⁸ As the short form of LKB1 has no normal nuclear localization signal, so it cannot form a tripolymer complex and fails to activate AMPK. Although mTOR signaling is an important negative regulator of autophagy and the AMPK/mTOR pathway can be activated by LKB1, the independence of cytoplasmic LKB1_s promoting autophagy suggests that cytoplasmic LKB1 might enhance autophagy by other pathways or stimuli. Actually, previous studies have shown that the Bcl-2 family,¹⁹ p53 protein,²⁰ oxidative stress,²¹ and endoplasmic reticulum stress²² can enhance autophagy. We are interested in further investigating the precise mechanisms underlying the action of LKB1_s in promoting cell autophagy and the growth of lung adenocarcinoma cells.

To look for clinical significance, we characterized LKB1 expression in 190 lung adenocarcinoma samples. We found that LKB1 was expressed in both the nucleus and cytoplasm of lung adenocarcinoma. Interestingly, the levels of nuclear LKB1 were inversely associated with cytoplasmic LKB1 in lung adenocarcinoma. Furthermore, cytoplasmic LKB1 was associated with poor OS in this population and was an independent risk factor for prognosis.

In summary, our data indicated that cytoplasmic LKB1 promoted A549 and HCC827 cell survival in vitro and in vivo. Furthermore, cytoplasmic LKB1 was associated with poor prognosis in lung adenocarcinoma cancer. Therefore, our findings could provide new insights into the pathogenesis of lung adenocarcinoma and novel biomarkers for prognosis of lung adenocarcinoma.

ACKNOWLEDGMENTS

This study was supported by the National Natural Science Foundation of China (Grant No. 81502099).

CONFLICT OF INTEREST

The authors have no conflict of interest.

5 | ETHICS APPROVAL

All protocols were approved by the Ethics Committee of Xi'an Jiaotong University, and informed consent was obtained from all patients before surgery. All in vivo protocols were approved by the Institutional Animal Care and Use Committee of Xi'an Jiaotong University.

ORCID

Mengjie Liu  <http://orcid.org/0000-0001-7823-1851>

REFERENCES

- Kohn L, Johansson M, Grankvist K, Nilsson J. Liquid biopsies in lung cancer-time to implement research technologies in routine care? *Ann Transl Med.* 2017;5(13):278.
- Shorning BY, Clarke AR. Energy sensing and cancer: LKB1 function and lessons learnt from Peutz-Jeghers syndrome. *Semin Cell Dev Biol.* 2016;52:21-29.
- Gupta R, Liu AY, Glazer PM, Wajapeyee N. LKB1 preserves genome integrity by stimulating BRCA1 expression. *Nucleic Acids Res.* 2015;43(1):259-271.
- Liu Y, Marks K, Cowley GS, et al. Metabolic and functional genomic studies identify deoxythymidylate kinase as a target in LKB1-mutant lung cancer. *Cancer Discov.* 2013;3(8):870-879.
- Li J, Liu J, Li P, et al. Loss of LKB1 disrupts breast epithelial cell polarity and promotes breast cancer metastasis and invasion. *J Exp Clin Cancer Res.* 2014;33:70.
- Morton JP, Jamieson NB, Karim SA, et al. LKB1 haploinsufficiency cooperates with Kras to promote pancreatic cancer through suppression of p21-dependent growth arrest. *Gastroenterology.* 2010;139(2):586-597. e1-6.
- Jiang L, Liang X, Liu M, et al. Reduced expression of liver kinase B1 and Beclin1 is associated with the poor survival of patients with non-small cell lung cancer. *Oncol Rep.* 2014;32(5):1931-1938.
- Ohsumi Y. Historical landmarks of autophagy research. *Cell Res.* 2014;24(1):9-23.
- Liuzzi JP, Guo L, Yoo C, Stewart TS. Zinc and autophagy. *Biometals.* 2014;27(6):1087-1096.
- Parzych KR, Klionsky DJ. An overview of autophagy: morphology, mechanism, and regulation. *Antioxid Redox Signal.* 2014;20(3):460-473.
- Gewirtz DA. The four faces of autophagy: implications for cancer therapy. *Cancer Res.* 2014;74(3):647-651.
- Yang F, Zhang L, Gao Z, et al. Exogenous H₂S protects against diabetic cardiomyopathy by activating autophagy via the AMPK/mTOR pathway. *Cell Physiol Biochem.* 2017;43(3):1168-1187.
- Han D, Li SJ, Zhu YT, Liu L, Li MX. LKB1/AMPK/mTOR signaling pathway in non-small-cell lung cancer. *Asian Pac J Cancer Prev.* 2013;14(7):4033-4039.
- Choi AM, Ryter SW, Levine B. Autophagy in human health and disease. *N Engl J Med.* 2013;368(19):1845-1846.
- Nikoletopoulou V, Markaki M, Palikaras K, Tavernarakis N. Crosstalk between apoptosis, necrosis and autophagy. *Biochim Biophys Acta.* 2013;1833(12):3448-3459.
- White E. The role for autophagy in cancer. *J Clin Invest.* 2015;125(1):42-46.
- Dong LX, Sun LL, Zhang X, et al. Negative regulation of mTOR activity by LKB1-AMPK signaling in non-small cell lung cancer cells. *Acta Pharmacol Sin.* 2013;34(2):314-318.

18. Zeqiraj E, Filippi BM, Deak M, Alessi DR, van Aalten DM. Structure of the LKB1-STRAD-MO25 complex reveals an allosteric mechanism of kinase activation. *Science*. 2009;326(5960):1707-1711.
19. McCarthy A, Marzec J, Clear A, et al. Dysregulation of autophagy in human follicular lymphoma is independent of overexpression of BCL-2. *Oncotarget*. 2014;5(22):11653-11668.
20. White E. Autophagy and p53. *Cold Spring Harb Perspect Med*. 2016;6(4):a026120.
21. Filomeni G, De Zio D, Cecconi F. Oxidative stress and autophagy: the clash between damage and metabolic needs. *Cell Death Differ*. 2015;22(3):377-388.
22. Lee WS, Yoo WH, Chae HJ. ER stress and autophagy. *Curr Mol Med*. 2015;15(8):735-745.

How to cite this article: Liu M, Jiang L, Fu X, et al. Cytoplasmic liver kinase B1 promotes the growth of human lung adenocarcinoma by enhancing autophagy. *Cancer Sci*. 2018;109:3055–3067. <https://doi.org/10.1111/cas.13746>